# Quadratic electronic response of a two-dimensional electron gas

A. Bergara and J. M. Pitarke

*Materia Kondentsatuaren Fisika Saila, Zientzi Fakultatea, Euskal Herriko Unibertsitatea, 644 Posta Kutxatila, 48080 Bilbo, Spain*

P. M. Echenique

*Materialen Fisika Saila, Kimika Fakultatea, Euskal Herriko Unibertsitatea, 1072 Posta Kutxatila, 20080 Donostia, Spain*

The electronic response of a two-dimensional (2D) electron system represents a key quantity in discussing one-electron properties of electrons in semiconductor heterojunctions, on the surface of liquid helium and in copper-oxide planes of high-temperature superconductors. We here report an evaluation of the wave-vector and frequency dependent dynamical quadratic density-response function of a 2D electron gas (2DEG), within a self-consistent field approximation. We use this result to find the $Z_1^3$ correction to the stopping power of a 2DEG for charged particles moving at a fixed distance from the plane of the 2D sheet, $Z_1$ being the projectile charge. We reproduce, in the high-density limit, previous full nonlinear calculations of the stopping power of a 2DEG for slow antiprotons, and we go further to calculate the $Z_1^3$ correction to the stopping power of a 2DEG for a wide range of projectile velocities. Our results indicate that linear-response calculations are, for all projectile velocities, less reliable in two dimensions than in three dimensions. [S0163-1829(99)00711-0]

## I. INTRODUCTION

Since the pioneering work of Bohm and Pines,[1] the conduction electrons in a metal have been described as a three-dimensional (3D) gas of electrons in a neutralizing uniform positive charge. The dynamical linear density-response function of a 3D electron gas (3DEG) was evaluated by Lindhard[2] in the so-called random-phase approximation (RPA), in which each electron is assumed to move in the external field plus the induced field of all electrons. The wave-vector and frequency dependent dynamical quadratic density-response function of a 3DEG has also been evaluated,[3] by going beyond linear response theory. The knowledge of this quantity has been proved to be of great importance in discussing the properties of electrons in a variety of 3D systems,[4] and, in particular, in explaining the experimentally observed difference between the electronic energy losses of protons and antiprotons moving through a solid.[5,6]

The suggested existence of two-dimensional electron layers in metal-insulator semiconductor structures and on the surface of liquid helium led several years ago to a great activity in the study of a two-dimensional electron gas,[7] where the electrons are confined to a plane and neutralized by an inert uniform rigid positive plane background. The 2D electron system has also been considered in discussing the physics of new-class materials such as copper-oxide planes of high-temperature superconductors.[8] It has been found that electrons confined to a 2D layer show sometimes interesting properties not shared by a 3D electron system. For instance, for a 2D metal the plasma frequency goes to zero in the long-wavelength limit, in contrast to the 3D situation.[9] Stern[10] evaluated the dynamical linear density-response function of a 2DEG in the RPA, and calculated the plasmon dispersion and the asymptotic screened Coulomb potential.

Also, much effort has gone into studying the ground-state energy[11] and the excitation spectrum of a 2DEG.[12] The stopping power for a fast particle moving parallel to a 2DEG was first evaluated in the RPA, within linear response theory, by Horing *et al.*,[13] and the effect on this quantity of finite temperature,[14] local field corrections,[15] and recoil[16] has also been considered. Nonlinear calculations of the stopping power for slow protons and antiprotons have been performed only very recently[17,18] on the basis of a scattering theory approach, the scattering cross sections being calculated for a statically screened potential.

In this paper we present results for the dynamical quadratic electronic density-response of a 2DEG to longitudinal external fields of arbitrary wave vector and frequency, which we evaluate on the same level of approximation as the RPA linear density-response function of Stern.[10] In order to illustrate the usefulness of the knowledge of this quantity, we consider, as an example, the stopping power of a 2DEG, and we use the quadratic density-response function to evaluate the $Z_1^3$ nonlinear correction to the stopping power of a 2DEG for particles of charge $Z_1 e$ moving at a fixed distance from the 2D plasma.

## II. DYNAMICAL ELECTRONIC RESPONSE

We consider a uniform electron system of density $n_0$ at zero temperature. Linear and quadratic density-response functions of this system, $\chi(x,x')$ and $Y(x,x',x'')$, with $x=(\mathbf{r},t)$, may be introduced in connection with the response to the presence of a time-varying external influence, after an expansion of the induced electron density in powers of the external potential $V(x)$. According to time-dependent perturbation theory, the induced electron density is given, up to second order in $V(x)$, by (we use atomic units throughout, i.e., $e^2 = \hbar = m_e = 1$)

$$n^{ind}(x) = \int dx' \chi(x,x') V(x')$$

$$+ \int dx' \int dx'' Y(x,x',x'') V(x') V(x''),$$

$$(2.1)$$

where

$$\chi(x,x') = -i\,\Theta(t-t') \langle \Psi_0 | [\tilde{\rho}_H(x), \tilde{\rho}_H(x')] | \Psi_0 \rangle \quad (2.2)$$

and

$$Y(x,x',x'') = \Theta(t-t')\Theta(t'-t'')$$

$$\times \langle \Psi_0 | \{ [\tilde{\rho}_H(x), \tilde{\rho}_H(x')], \tilde{\rho}_H(x'') \} | \Psi_0 \rangle / 2$$

$$+ \Theta(t-t'')\Theta(t''-t')$$

$$\times \langle \Psi_0 | \{ [\tilde{\rho}_H(x), \tilde{\rho}_H(x'')], \tilde{\rho}_H(x') \} | \Psi_0 \rangle / 2.$$

$$(2.3)$$

Here $|\Psi_0\rangle$ denotes the normalized ground state, $\tilde{\rho}_H$ is the density fluctuation operator $\tilde{\rho}_H = \hat{\rho}_H - n_0$, where $\hat{\rho}_H$ is the exact Heisenberg density operator in the unperturbed system, and $\Theta(x)$ is the Heaviside step function accounting for causality.

In a self-consistent field or random-phase approximation (RPA), it is assumed that the electron density induced by an external potential can be replaced by the electron density induced in a noninteracting electron gas by the sum of the external potential, $V(x)$, and the potential created by the induced electron density itself, $V^{ind}(x)$. Hence, in this approximation,

$$n^{ind}(x) = \int dx' \chi^0(x,x') [V(x') + V^{ind}(x')]$$

$$+ \int dx' \int dx'' Y^0(x,x',x'') [V(x') + V^{ind}(x')]$$

$$\times [V(x'') + V^{ind}(x'')].$$

$$(2.4)$$

Here $\chi^0(x,x')$ and $Y^0(x,x',x'')$ are ''free-particle'' linear and quadratic density-response functions, and

$$V^{ind}(x) = \int dx' v(x,x') n^{ind}(x'), \quad (2.5)$$

where $v(x,x')$ represents the instantaneous Coulomb interaction. Introducing Eq. (2.5) into Eq. (2.4) and keeping in Eq. (2.4) only terms up to second order in $V(x)$, one finds the following integral equations for RPA linear and quadratic density-response functions:

$$\chi(x_1,x_2) = \chi^0(x_1,x_2)$$

$$+ \int dx_1' \int dx_2' \chi^0(x_1,x_1') v(x_1',x_2') \chi(x_2',x_2)$$
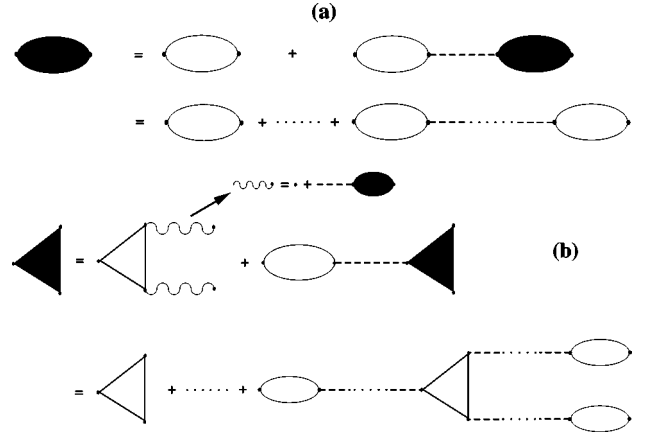
$$(2.6)$$

and



FIG. 1. Diagrammatic interpretation of the RPA integral Eqs. (2.6) and (2.7) for (a) linear and (b) quadratic density-response functions, respectively. Electron-hole empty and full bubbles represent noninteracting and interacting linear density-response functions, respectively. Empty and full triangles represent noninteracting and interacting quadratic density-response functions, respectively. The interacting RPA quadratic density-response function is obtained by summing over the infinite set of diagrams that combine three strings of empty bubbles (two-electron loops) through an empty three-electron loop. Dashed lines represent the electron-electron bare Coulomb interaction.

$$Y(x_1,x_2,x_3)$$

$$= \int dx_2' \int dx_3' Y^0(x_1,x_2',x_3') K(x_2',x_2) K(x_3',x_3)$$

$$+ \int dx_1' \int dx_1'' \chi^0(x_1,x_1') v(x_1',x_1'') Y(x_1'',x_2,x_3),$$

$$(2.7)$$

where $K(x,x')$ is the so-called inverse dielectric function:

$$K(x,x') = \delta(x-x') + \int dx'' v(x,x'') \chi(x'',x'). \quad (2.8)$$

The integral Eqs. (2.6) and (2.7) have, within many-body perturbation theory, the simple diagrammatic interpretation shown in Fig. 1, where empty and full bubbles represent noninteracting and interacting linear density-response functions $\chi^0(x_1,x_2)$ and $\chi(x_1,x_2)$, respectively. Similarly, empty and full triangles represent noninteracting and interacting quadratic density-response functions $Y^0(x_1,x_2,x_3)$ and $Y(x_1,x_2,x_3)$, respectively, and dashed lines represent the Coulomb interaction $v(x,x')$. Thus, RPA linear and quadratic density-response functions are represented diagrammatically by summing over the infinite set of diagrams containing one [see Fig. 1(a)] and three [see Fig. 1(b)] strings of empty bubbles, respectively.

In the case of a homogeneous 2DEG, the electrons are free to move in two spatial dimensions, having their motion constrained in the third dimension. Thus, assuming time invariance, we define the Fourier transforms

$$\chi_q = \int d^2\mathbf{r}_1 \int dt_1 e^{-i[\mathbf{q}\cdot(\mathbf{r}_1-\mathbf{r}_2)-\omega(t_1-t_2)]} \chi(\mathbf{r}_1,t_1;\mathbf{r}_2,t_2)$$

$$(2.9)$$

and

$$Y_{q_1,q_2} = \int d^2\mathbf{r}_1 \int dt_1 \int d^2\mathbf{r}_2 \int dt_2 e^{-i[\mathbf{q}_1\cdot(\mathbf{r}_1-\mathbf{r}_2)-\omega_1(t_1-t_2)]} e^{-i[(\mathbf{q}_1+\mathbf{q}_2)\cdot(\mathbf{r}_2-\mathbf{r}_3)-(\omega_1+\omega_2)(t_2-t_3)]} Y(\mathbf{r}_1,t_1;\mathbf{r}_2,t_2;\mathbf{r}_3,t_3),$$

(2.10)

where $\mathbf{r}_1,\mathbf{r}_2$, and $\mathbf{r}_3$ represent two-dimensional position vectors in the 2D plane, and $q$ is the trimomentum $q=(\mathbf{q},q^0)$. Hence within the RPA we find

$$\chi_q = \chi_q^0 + \chi_q^0 v_q \chi_q$$

(2.11)

and

$$Y_{q,-q_1} = Y_{q,-q_1}^0 K_{q_1} K_{q-q_1} + \chi_q^0 v_q Y_{q,-q_1},$$

(2.12)

where

$$K_q = 1 + v_q \chi_q$$

(2.13)

and $v_q = 2\pi/|\mathbf{q}|$.

For a noninteracting Fermi gas, the ground state is obtained by filling all the plane-wave states inside the Fermi sphere of radius $q_F = \sqrt{2}/r_s$, $r_s$ being the average interelectronic distance ($n_0^{-1} = \pi r_s^2$). As in the case of a 3DEG,[19] we find noninteracting linear and quadratic density-response functions to be[20]

$$\chi_q^0 = 2\int \frac{d^2\mathbf{k}}{(2\pi)^2}\left[\frac{n_\mathbf{k}(1-n_{\mathbf{k}+\mathbf{q}})}{q^0-(\omega_{\mathbf{k}+\mathbf{q}}-\omega_\mathbf{k})+i\eta} + \frac{(1-n_\mathbf{k})n_{\mathbf{k}+\mathbf{q}}}{-q^0-(\omega_\mathbf{k}-\omega_{\mathbf{k}+\mathbf{q}})-i\eta}\right]$$

(2.14)

and

$$Y_{q,-q_1}^0 = -\int \frac{d^2\mathbf{k}}{(2\pi)^2}\left[\frac{n_\mathbf{k}(1-n_{\mathbf{k}+\mathbf{q}})(1-n_{\mathbf{k}+\mathbf{q}_1})}{(q^0+\omega_\mathbf{k}-\omega_{\mathbf{k}+\mathbf{q}}+i\eta)(q_1^0+\omega_\mathbf{k}-\omega_{\mathbf{k}+\mathbf{q}_1}+i\eta)} - \frac{(1-n_\mathbf{k})n_{\mathbf{k}+\mathbf{q}}n_{\mathbf{k}+\mathbf{q}_1}}{(q^0+\omega_\mathbf{k}-\omega_{\mathbf{k}+\mathbf{q}}+i\eta)(q_1^0+\omega_\mathbf{k}-\omega_{\mathbf{k}+\mathbf{q}_1}+i\eta)}\right.$$

$$+ \frac{n_{\mathbf{k}+\mathbf{q}}(1-n_\mathbf{k})(1-n_{\mathbf{k}+\mathbf{q}_1})}{(-q^0+\omega_{\mathbf{k}+\mathbf{q}}-\omega_\mathbf{k}-i\eta)(-q^0+q_1^0+\omega_{\mathbf{k}+\mathbf{q}}-\omega_{\mathbf{k}+\mathbf{q}_1}-i\eta)}$$

$$- \frac{(1-n_{\mathbf{k}+\mathbf{q}})n_\mathbf{k}n_{\mathbf{k}+\mathbf{q}_1}}{(-q^0+\omega_{\mathbf{k}+\mathbf{q}}-\omega_\mathbf{k}-i\eta)(-q^0+q_1^0+\omega_{\mathbf{k}+\mathbf{q}}-\omega_{\mathbf{k}+\mathbf{q}_1}-i\eta)}$$

$$+ \frac{n_{\mathbf{k}+\mathbf{q}_1}(1-n_\mathbf{k})(1-n_{\mathbf{k}+\mathbf{q}})}{(-q_1^0+\omega_{\mathbf{k}+\mathbf{q}_1}-\omega_\mathbf{k}-i\eta)(q^0-q_1^0+\omega_{\mathbf{k}+\mathbf{q}_1}-\omega_{\mathbf{k}+\mathbf{q}}+i\eta)} - \frac{(1-n_{\mathbf{k}+\mathbf{q}_1})n_\mathbf{k}n_{\mathbf{k}+\mathbf{q}}}{(-q_1^0+\omega_{\mathbf{k}+\mathbf{q}_1}-\omega_\mathbf{k}-i\eta)(q^0-q_1^0+\omega_{\mathbf{k}+\mathbf{q}_1}-\omega_{\mathbf{k}+\mathbf{q}}+i\eta)}$$

$$\left. + (q_1\rightarrow q-q_1)\right],$$

(2.15)

where $n_\mathbf{q} = \Theta(q_F-|\mathbf{q}|)$, $\omega_\mathbf{k} = \mathbf{k}^2/2$, and $\eta$ is a positive infinitesimal.

Analytical evaluation of Eq. (2.14) results in the noninteracting linear density-response function of Stern.[10] As for the noninteracting quadratic density-response function, we first sum occupation numbers in Eq. (2.15) to find

$$Y_{q,-q_1}^0 = -\int \frac{d^2\mathbf{k}}{(2\pi)^2} n_\mathbf{k}\left[\frac{1}{q^0+\omega_\mathbf{k}-\omega_{\mathbf{k}+\mathbf{q}}+i\eta}\frac{1}{q_1^0+\omega_\mathbf{k}-\omega_{\mathbf{k}+\mathbf{q}_1}+i\eta} + \frac{1}{-q^0+\omega_\mathbf{k}-\omega_{\mathbf{k}+\mathbf{q}}-i\eta}\frac{1}{-(q^0-q_1^0)+\omega_\mathbf{k}-\omega_{\mathbf{k}+\mathbf{q}-\mathbf{q}_1}-i\eta}\right.$$

$$\left. + \frac{1}{-q_1^0+\omega_\mathbf{k}-\omega_{\mathbf{k}+\mathbf{q}_1}-i\eta}\frac{1}{(q^0-q_1^0)+\omega_\mathbf{k}-\omega_{\mathbf{k}-(\mathbf{q}-\mathbf{q}_1)}+i\eta} + (q_1\rightarrow q-q_1)\right].$$

(2.16)

For the real part, we find[21]

$$\mathrm{Re}[Y_{q,-q_1}^0] = -[(I_{q,q_1}+I_{q,q_1}') + (I_{-q,-q+q_1}+I_{-q,-q+q_1}') + (I_{-q_1,q-q_1}-I_{q_1,q-q_1}')],$$

(2.17)

where

$$I_{q,q_1} = \frac{1}{2\pi|\mathbf{q}||\mathbf{q}_1|\sin\chi}\left\{\arctan\left[\frac{A\sin\chi}{A_1-A\cos\chi}\right]\right.$$

$$-\operatorname{sgn}A\arctan\left[\frac{\sin\chi\sqrt{A^2-q_F^2}}{A_1-A\cos\chi}\right]\Theta(A^2-q_F^2)$$

$$+\arctan\left[\frac{A_1\sin\chi}{A-A_1\cos\chi}\right]$$

$$\left.-\operatorname{sgn}A_1\arctan\left[\frac{\sin\chi\sqrt{A_1^2-q_F^2}}{A-A_1\cos\chi}\right]\Theta(A^2-q_F^2)\right\} \quad (2.18)$$

and

$$I'_{q,q_1} = -\Theta(q_F^2\sin^2\chi-G)\frac{1}{4|\mathbf{q}||\mathbf{q}_1|\sin\chi}. \quad (2.19)$$

Here $A=q^0/|\mathbf{q}|-|\mathbf{q}|/2$, $A_1=q_1^0/|\mathbf{q}_1|-|\mathbf{q}_1|/2$, and $G=\sqrt{A^2-2AA_1\cos\chi+A_1^2}$, $\chi$ being the angle between $\mathbf{q}$ and $\mathbf{q}_1$.

As for the imaginary part of $Y_{q,-q_1}^0$ we define[5,6] the function $H_{q,q_1}$, which can be represented in terms of a sum over hole and particle states and gives the second-order contribution to the so-called absorption probability, as demonstrated in Ref. 6. We find

$$\operatorname{Im}[Y_{q,-q_1}^0]=H_{q,q_1}+H_{q_1,q}+H_{q-q_1,-q_1}, \quad (2.20)$$

where[21]

$$H_{q,q_1}=\frac{1}{2}[f_{q,q_1}-f_{-q,-q+q_1}+(q_1\to q-q_1)] \quad (2.21)$$

and

$$f_{q,q_1}=\Theta(q_F^2-A^2)\frac{1}{2\pi|\mathbf{q}||\mathbf{q}_1|\sin\chi}$$

$$\times\ln\left|\frac{A_1-A\cos\chi+\sin\chi\sqrt{q_F^2-A^2}}{A_1-A\cos\chi-\sin\chi\sqrt{q_F^2-A^2}}\right|. \quad (2.22)$$

In particular, at low frequencies an expansion of $H_{q,q_1}$ in powers of the frequency $q^0$ gives, after retaining only the first-order terms,

$$H_{q,q_1}^L=\Theta(4q_F^2-|\mathbf{q}|^2)$$

$$\times\frac{4(|\mathbf{q}|\cos\chi-|\mathbf{q}_1|)}{\pi|\mathbf{q}||\mathbf{q}_1|[|\mathbf{q}-\mathbf{q}_1|^2-4q_F^2\sin^2\chi]\sqrt{4q_F^2-|\mathbf{q}|^2}}q^0. \quad (2.23)$$

In the static limit ($q^0\to0$) both first- and second-order contributions to the absorption probability $\operatorname{Im}\chi_q$ and $H_{q,q_1}$ are proportional to the frequency $q^0$, as in the case of a 3DEG.

### III. ELECTRONIC STOPPING POWER

We consider an ion of charge $Z_1$ moving with constant velocity $\mathbf{v}$ at a fixed distance $h$ from a 2DEG of density $n_0$.

The Coulomb potential of this moving particle has the form

$$V(\mathbf{r},z;t)=Z_1|\mathbf{r}-\mathbf{v}t+(z-h)\hat{\mathbf{k}}|^{-1}, \quad (3.1)$$

where $\mathbf{r}$ represents, as in Eqs. (2.9) and (2.10), a two-dimensional position vector in the 2D plane, and $z$ denotes the coordinate normal to the 2DEG which we consider to be located at $z=0$. Hence, in order to obtain the induced potential, we introduce this time-varying external potential into Eq. (2.1), and Eq. (2.1) into Eq. (2.5). We note that density-response functions of a 2DEG have their $z$ arguments localized to the 2D plane by positional $\delta$ functions, we Fourier transform, and find, up to second order in $Z_1$,

$$V^{ind}(\mathbf{r},z;t)=Z_1\int\frac{d^2\mathbf{q}}{(2\pi)^2}e^{i(\mathbf{q}\cdot\mathbf{r}-\omega t)-|\mathbf{q}|(|z|+h)}v_\mathbf{q}\chi_{\mathbf{q},\omega}v_\mathbf{q}$$

$$+Z_1^2\int\frac{d^2\mathbf{q}}{(2\pi)^2}\int\frac{d^2\mathbf{q}_1}{(2\pi)^2}$$

$$\times e^{i(\mathbf{q}\cdot\mathbf{r}-\omega t)-[|\mathbf{q}||z|+(|\mathbf{q}_1|+|\mathbf{q}-\mathbf{q}_1|)h]}$$

$$\times v_\mathbf{q}Y_{\mathbf{q},\omega;-\mathbf{q}_1,-\omega_1}v_{\mathbf{q}_1}v_{\mathbf{q}-\mathbf{q}_1}, \quad (3.2)$$

where $\omega=\mathbf{q}\cdot\mathbf{v}$ and $\omega_1=\mathbf{q}_1\cdot\mathbf{v}$.

The stopping power of the 2DEG is simply the retarding force that the polarization charge distribution in the vicinity of the projectile exerts on the projectile itself,[22] and is given by

$$S=\frac{Z_1}{v}\int d^2\mathbf{r}\int dz\,\delta(\mathbf{r}-\mathbf{v}t)\,\delta(z-h)\nabla V^{ind}(\mathbf{r},z;t)\cdot\mathbf{v}. \quad (3.3)$$

Substituting Eq. (3.2) into Eq. (3.3), we have[23]

$$S=-\frac{Z_1^2}{v}\int\frac{d^2\mathbf{q}}{(2\pi)^2}\omega e^{-2|\mathbf{q}|h}v_\mathbf{q}\operatorname{Im}[\chi_{\mathbf{q},\omega}]v_\mathbf{q}$$

$$-\frac{Z_1^3}{v}\int\frac{d^2\mathbf{q}}{(2\pi)^2}\omega\int\frac{d^2\mathbf{q}_1}{(2\pi)^2}e^{-(|\mathbf{q}|+|\mathbf{q}_1|+|\mathbf{q}-\mathbf{q}_1|)h}v_\mathbf{q}$$

$$\times\operatorname{Im}[Y_{\mathbf{q},\omega;-\mathbf{q}_1,-\omega_1}]v_{\mathbf{q}_1}v_{\mathbf{q}-\mathbf{q}_1}. \quad (3.4)$$

In the RPA, $\chi_q$ and $Y_{q,-q_1}$ are obtained from Eqs. (2.11) and (2.12) or, equivalently, from

$$v_q\chi_q=K_q-1 \quad (3.5)$$

and

$$Y_{q,-q_1}=K_qY_{q,-q_1}^0K_{q_1}K_{q-q_1}, \quad (3.6)$$

where

$$K_q=(1-\chi_q^0v_q)^{-1}. \quad (3.7)$$

The linear contribution to the stopping power of Eq. (3.4), which is proportional to $Z_1^2$, was evaluated in the RPA by Horing *et al.*[13] at $T=0$, and similar calculations were presented by Bret and Deutsch[14] at finite temperature. On the other hand, the quadratic contribution to the stopping power of Eq. (3.4) is, in the RPA and for a geometry with the

ion-beam in plane within the 2D electron layer ($h=0$), equivalent to the result derived in Ref. 6, within many-body perturbation theory, as the energy loss per unit path length of the projectile, the integration space being now in two dimensions instead of three dimensions. This contribution to the stopping power, which is proportional to $Z_1^3$, discriminates between the energy loss of a proton and that of an antiproton, and appears as a consequence of losses to one- and two-step electronic excitations generated by both linearly and quadratically screened ion potentials, as discussed in Ref. 6.

In the case of slow intruders ($v \rightarrow 0$), only the low-frequency form of the response enters in the evaluation of Eq. (3.4). At zero frequencies both linear and quadratic density-response functions are real, Im[$\chi_q^0$] and $H_{q,q_1}$ being at low frequencies proportional to the frequency $q^0$. Thus retaining only the first-order terms in the frequencies, both $Z_1^2$ and $Z_1^3$ contributions to the stopping power are found to be proportional to the velocity of the projectile, as in a 3DEG. For the RPA quadratic contribution to the stopping power we find, after insertion of Eq. (2.23) into Eq. (3.4), the following result:

$$[S^L]^{(3)} = 8vZ_1^3 \int_0^\infty \frac{d|\mathbf{q}|}{\sqrt{4q_F^2 - |\mathbf{q}|^2}} \int_0^\infty d|\mathbf{q}_1|$$

$$\times \int_0^\pi d\chi e^{-(|\mathbf{q}| + |\mathbf{q}_1| + |\mathbf{q} - \mathbf{q}_1|)h} \frac{f_1^L + f_2^L}{|\mathbf{q} - \mathbf{q}_1|}, \quad (3.8)$$

where

$$f_1^L = \Theta(2q_F - |\mathbf{q}|)K_{\mathbf{q},0}^2 K_{\mathbf{q}_1,0}K_{\mathbf{q}-\mathbf{q}_1,0}Y_{\mathbf{q},0;\mathbf{q}_1,0}^0 \quad (3.9)$$

and

$$f_2^L = -\Theta(2q_F - |\mathbf{q}|)$$

$$\times \frac{|\mathbf{q}|(|\mathbf{q}|\cos\chi - |\mathbf{q}_1|)}{\pi|\mathbf{q}_1|(|\mathbf{q}-\mathbf{q}_1|^2 - 4q_F^2\sin^2\chi)}K_{\mathbf{q},0}K_{\mathbf{q}_1,0}K_{\mathbf{q}-\mathbf{q}_1,0}.$$

$$(3.10)$$

## IV. RESULTS

In the low-velocity limit ($v \rightarrow 0$), the stopping power can be evaluated to all orders in $Z_1$, on the basis of a free-electron picture, with the additional assumption of independent, individual, elastic electron scattering, and it is easily found to be, in both two and three dimensions, proportional to the velocity of the projectile.[24] By using density-functional theory (DFT) (Ref. 25) to calculate the self-consistent potential generated by a static charge submerged in a 3DEG, Echenique *et al.*[26] evaluated the nonlinear stopping power of a 3DEG for slow ions. Nonlinear calculations for an in-plane projectile in 2D have been performed recently by using a nonlinearly screened scattering potential based on the Sjölander-Stott theory,[17] with the use of a nonlinear version of the linearized Fermi-Thomas potential[18] in which the screening constant is determined from the Friedel sum rule,
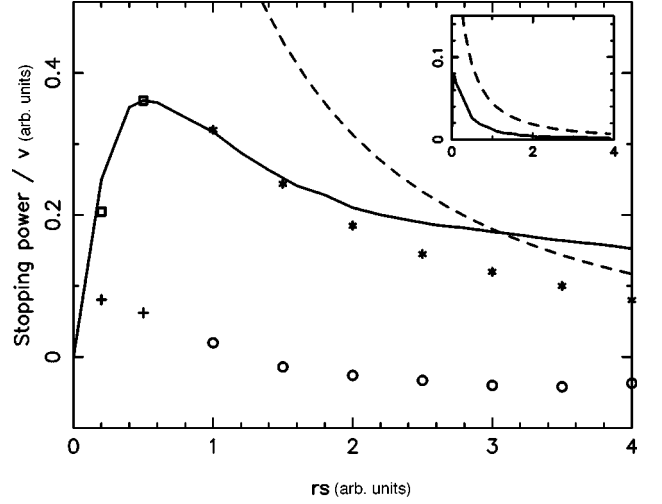


FIG. 2. Low-velocity limit of the $Z_1^3$ stopping power, as obtained from Eq. (3.8) (solid line) for $h=0$ and $Z_1=1$, divided by the velocity, as a function of $r_s$; the corresponding $Z_1^2$ stopping power is represented by a dashed line. Full nonlinear contributions to the stopping power for antiprotons ($Z_1=-1$) (stars and squares) and protons ($Z_1=1$) (circles and crosses) have been obtained by subtracting RPA linear calculations from the results of Ref. 18 (stars and circles) and Ref. 27 (with XC contributions to the DFT scattering potential excluded) (squares and crosses), and dividing by $Z_1$; thus, the negative values at $r_s>1$ simply mean that the full nonlinear stopping power lies, in the case of protons, below the linear results. The inset exhibits $Z_1^2$ and $Z_1^3$ contributions to the stopping power (dashed and solid lines, respectively) for $h=1/q_F$ and $Z_1=1$.

and on the basis of a self-consistent potential[27] obtained within DFT as in Ref. 26 for the 3D case.

The nonlinear calculations presented in Ref. 18 for the energy loss of slow protons and antiprotons are very close to the calculations of Ref. 27 when exchange and correlation (XC) contributions to the DFT scattering potential are excluded. These calculations are correct to all orders in $Z_1$, and they represent, therefore, a good check for our quadratic response calculations, which should be exact in the high-density and/or low $Z_1$ limits. Nevertheless, the approaches of Refs. 17, 18, and 27 have the limitation of being restricted to very low ion velocities ($v \ll v_F$, $v_F$ being the Fermi velocity), while our nonlinear $Z_1^3$ corrections are valid for arbitrary nonrelativistic velocities.

The low-velocity limit of the quadratic stopping power, as obtained from Eq. (3.8) for an in-plane ($h=0$) moving charge and divided by the velocity, is represented in Fig. 2 by a solid line, as a function of the electron-density parameter $r_s$. Stars and squares represent the full nonlinear contribution to the stopping power for antiprotons reported in Refs. 18 and 27, respectively, multiplied by a factor of $-1$, showing an excellent agreement, in the high-density limit, with our $Z_1^3$ nonlinear contribution. For $r_s \geq 2$, higher-order corrections become important, and for $r_s>3$, $Z_1^2$ contributions (dashed line) are smaller than the $Z_1^3$ correction, indicating that the external potential cannot be treated, for these electron densities, as a small perturbation. In the case of a projectile moving at a given $h$ distance above the 2D plasma the external perturbation is obviously diminished and, in par-
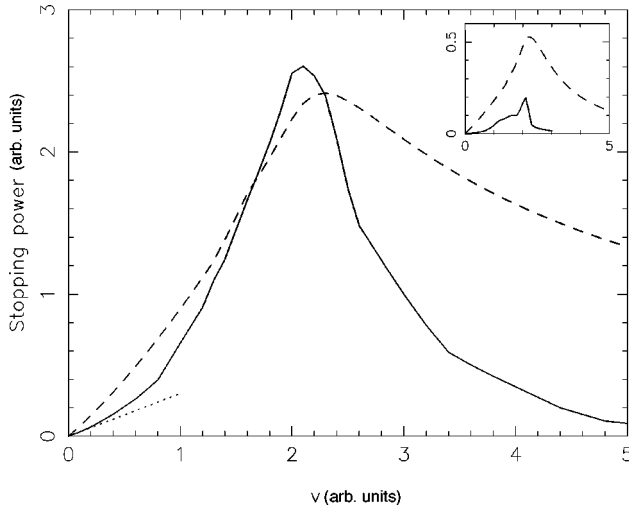
FIG. 3. Full RPA $Z_1^3$ stopping power, as obtained from Eq. (3.4) (solid line) for $Z_1 = 1$, $h = 0$, and $r_s = 1$, as a function of the velocity of the projectile. The corresponding $Z_1^2$ stopping power is represented by a dashed line, and the dotted line represents the low-velocity limit of the $Z_1^3$ term. The inset shows the same results for $h = 1/q_F$.

ticular, for $h = 1/q_F$ the quadratic stopping power is smaller than the linear one for all electron densities (see the inset of Fig. 2). The full nonlinear contribution to the stopping power for protons reported in Refs. 18 and 27 for $h = 0$ is also represented in Fig. 2 by circles and crosses, respectively, showing large differences with our $Z_1^3$ calculations for all electron densities. These differences appear as a consequence of perturbation theory failing to describe electronic states bound to the proton, which in 2D systems can be supported by arbitrarily weak attractive potentials.[28]

As the velocity of the projectile ($v$) and/or the distance from the 2D plasma ($h$) increase, the ion potential becomes a relatively smaller perturbation and the $Z_1^3$ contribution to the stopping power for antiprotons may, therefore, be expected to approximately describe the full nonlinear contribution to the stopping power for arbitrary values of $v$ and $h$, as long as $r_s < 2$, and also for lower densities ($r_s \geq 2$) as the velocity and the $h$ distance increase. Substitution of the full RPA linear and quadratic 2DEG density-response functions of Eqs. (3.5) and (3.6) into Eq. (3.4) results in the quadratic stopping power plotted by a solid line in Fig. 3, as a function of the impinging projectile velocity, for $r_s = 1$ and $h = 0$, and also for $r_s = 1$ and $h = 1/q_F$ (see the inset of Fig. 3). The dotted line represents the low-velocity limit, as obtained from Eq. (3.8), and dashed lines represent linear RPA contributions to the stopping power of Eq. (3.4).

The quadratic contribution to the stopping power of a 2DEG presents properties not shared by the 3DEG. First, the range of validity of the linear velocity dependence of this contribution to the stopping power (see Fig. 3) persists only up to velocities much smaller than the Fermi velocity, in contrast to the 3D situation in which the linear velocity dependence persists up to velocities approaching the Fermi velocity.[6] Second, at velocities around the plasmon threshold velocity, for which the projectile has enough energy to excite a plasmon,[29] the ratio between $Z_1^3$ and $Z_1^2$ contributions to the stopping power increases, again in contrast to the 3D situa-
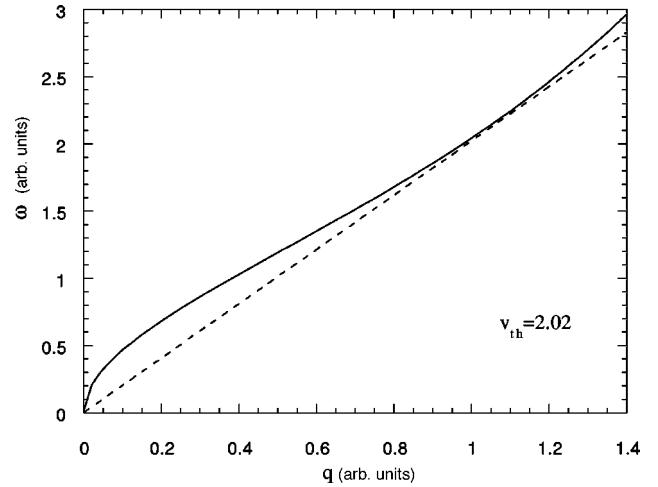


FIG. 4. Two-dimensional RPA plasmon dispersion relation (solid line) and maximum energy transfer ($\omega_{max} = qv$) at the plasmon threshold velocity (dotted line), as functions of the wave number. The electron density parameter has been taken to be $r_s = 1$, thus the plasmon threshold velocity being $v_{th} = 2.02$ $v_0$ ($v_0$ is Bohr's velocity).

tion. Furthermore, we have found that the increase of this ratio at the plasmon threshold velocity becomes dramatic as the electron density decreases. Of course, the ratio between quadratic and linear contributions to the stopping power decreases very rapidly with $h$ (see the inset of Fig. 3), but the relative, and for large $r_s$ dramatic, increase of this ratio at the plasmon threshold velocity persists for all values of $h$ that are not much larger than $1/q_F$. For a 2DEG the group velocity of the plasmon wave nearly coincides with the plasmon threshold velocity of the projectile (see Fig. 4); also, the inclusion of short-range correlations, which are ignored in the RPA, is known to have a substantial effect on the plasmon dispersion.[30] We interpret the anomalous enhancement of the ratio between quadratic and linear contributions to the stopping power at the plasmon threshold velocity and small electron densities ($r_s > 1$) as a result of neglecting, within the RPA, short-range correlations between the electrons of a 2D system, since these correlations are non-negligible for all values of $h$ as long as $r_s$ is not small.

## V. CONCLUSIONS

We have presented an analytical evaluation of the wave-vector and frequency dependent noninteracting quadratic density-response function of a 2DEG. We have used this result to find, within a self-consistent field approximation, the $Z_1^3$ correction to the stopping power of a 2DEG for charged recoilless particles moving at a fixed distance from the 2D plasma sheet. We have reproduced, in the high-density limit, previous full nonlinear calculations of the stopping power of a 2DEG for slow antiprotons, and we have gone further to calculate the $Z_1^3$ correction to the stopping power for a wide range of projectile velocities. We have found that the $Z_1^3$ contribution to the stopping power of a 2DEG presents properties not shared by the 3DEG. On the one hand, the range of validity of the linear velocity dependence of the $Z_1^3$ contribution to the stopping power persists only up to velocities much smaller than the Fermi velocity,

and, on the other hand, an anomalous enhancement of the ratio between quadratic and linear contributions to the stopping power at the plasmon threshold velocity is found, within the RPA, at small electron densities ($r_s > 1$). Also, our results indicate that linear response calculations are, for all projectile velocities, less reliable in two dimensions than in three dimensions.

[1] D. Bohm and D. Pines, Phys. Rev. **92**, 609 (1953).

[2] J. Lindhard, K. Dan. Vidensk. Selsk. Mat. Fys. Medd. **28**, 1 (1954).

[3] R. Cenni and P. Saracco, Nucl. Phys. A **487**, 279 (1988).

[4] C. F. Richardson and N. W. Ashcroft, Phys. Rev. B **50**, 8170 (1994); J. M. Rommel and G. Kalman, Phys. Rev. E **54**, 3518 (1996).

[5] J. M. Pitarke, R. H. Ritchie, P. M. Echenique, and E. Zaremba, Europhys. Lett. **24**, 613 (1993); J. M. Pitarke, R. H. Ritchie, and P. M. Echenique, Nucl. Instrum. Methods Phys. Res. B **24**, 613 (1993).

[6] J. M. Pitarke, R. H. Ritchie, and P. M. Echenique, Phys. Rev. B **52**, 13 883 (1995).

[7] T. Ando, A. Fowler, and F. Stern, Rev. Mod. Phys. **54**, 437 (1982).

[8] J. R. Engelbrecht and M. Randeria, Phys. Rev. Lett. **65**, 1032 (1990); P. W. Anderson, *ibid.* **64**, 1839 (1990).

[9] R. H. Ritchie, Phys. Rev. **106**, 874 (1957); Surf. Sci. **34**, 1 (1973).

[10] F. Stern, Phys. Rev. Lett. **18**, 546 (1967).

[11] A. K. Rajagopal and J. C. Kimball, Phys. Rev. B **15**, 2819 (1977).

[12] A. V. Chaplik, Zh. Eksp. Teor. Fiz. **60**, 1845 (1971); G. F. Giuliani, and J. J. Quinn, Phys. Rev. B **26**, 4421 (1982); L. Zheng and S. Das Sarma, *ibid.* **53**, 9964 (1996).

[13] N. J. M. Horing, H. C. Tso, and G. Gumbs, Phys. Rev. B **36**, 1588 (1987).

[14] A. Bret and C. Deutsch, Phys. Rev. E **48**, 2994 (1993).

[15] Y.-N. Wang and T.-C. Ma, Phys. Lett. A **200**, 319 (1995).

[16] A. Bergara, I. Nagy, and P. M. Echenique, Phys. Rev. B **55**, 12 864 (1997).

[17] A. Krakovsky and J. K. Percus, Phys. Rev. B **52**, R2305 (1995).

[18] Y.-N. Wang and T.-C. Ma, Phys. Rev. A **55**, 2087 (1997).

[19] C. D. Hu and E. Zaremba, Phys. Rev. B **37**, 9268 (1988); A. Bergara, I. Campillo, J. M. Pitarke, and P. M. Echenique, *ibid.* **56**, 15 654 (1997).

[20] Differences between the retarded density-response functions of Eqs. (2.14) and (2.15), on the one hand, and time-ordered response functions, as defined within many-body theory [see, e.g., G. D. Mahan, *Many-Particle Physics* (Plenum, New York, 1981)], on the other hand, lie in $\omega + i\eta$, which should be replaced in Eqs. (2.14) and (2.15) by $\omega + i\eta \, \mathrm{sgn}(\omega)[\omega$ being either $q^0, q_1^0$ or $(q^0 - q_1^0)]$ in order to obtain their time-ordered counterparts.

[21] $I'_{q,q_1}, I'_{-q,-q+q_1}$, and $I'_{-q_1,q-q_1}$ in Eq. (2.17) should be multiplied by $\mathrm{sgn}(q^0)\mathrm{sgn}(q_1^0)$, $\mathrm{sgn}(q^0)\mathrm{sgn}(q^0 - q_1^0)$, and $\mathrm{sgn}(q_1^0)\mathrm{sgn}(q^0 - q_1^0)$, respectively, to obtain the real part of the corresponding time-ordered quadratic response function. Similarly, the right-hand side of Eq. (2.21) should be multiplied by $\mathrm{sgn}(q^0)$ in order to obtain the imaginary part of the time-ordered quadratic response function.

[22] P. M. Echenique, F. Flores, and R. H. Ritchie, Solid State Phys. **43**, 229 (1990).

[23] The real parts of $\chi_q$ and $Y_{q,-q_1}$ give no contribution to the integrals of Eq. (3.4), since $\mathrm{Re}[\chi_q] = \mathrm{Re}[\chi_{-q}]$ and $\mathrm{Re}[Y_{q,q_1}] = \mathrm{Re}[Y_{-q,-q_1}]$.

[24] I. Nagy, Phys. Rev. B **51**, 77 (1995).

[25] P. Hohenberg and W. Kohn, Phys. Rev. **136**, B864 (1964); W. Kohn and L. J. Sham, Phys. Rev. **140**, A1133 (1965).

[26] P. M. Echenique, R. M. Nieminen, and R. H. Ritchie, Solid State Commun. **37**, 779 (1981); P. M. Echenique, R. M. Nieminen, J. C. Ashley, and R. H. Ritchie, Phys. Rev. A **33**, 897 (1986).

[27] E. Zaremba, P. M. Echenique, and I. Nagy (unpublished).

[28] E. N. Economou, *Green's Functions in Quantum Physics* (Springer-Verlag, Berlin, 1990), p. 64.

[29] At long wavelengths the plasma frequency in the 2DEG varies like $q^{1/2}$, in contrast to the 3D case [see, e. g., A. L. Fetter, Ann. Phys. (N.Y.) **81**, 367 (1973)]. At short wavelengths, the group velocity of the 2D plasmon is nearly constant and approaches the plasmon threshold velocity, $v_{\mathrm{th}}$. For $r_s = 1, v_{\mathrm{th}} = 2.02 v_0$ ($v_0$ is Bohr's velocity).

[30] A. Gold and L. Calmels, Phys. Rev. B **48**, 11 622 (1993).